Journal of Environmental Protection and Ecology 21, No 4, 1298–1313 (2020)

Environmental protection and sustainable development

METHOD AND DEVICE FOR THE STUDY OF DAMPING OF ENVIRONMENTAL FRIENDLY FOAM TYPE MATERIALS

S. ALACI[a]*, ZH. KALITCHIN[b], M. KANDEVA[c,d], F. C. CIORNEI[a]

[a]*Mechanics and Technologies Department, Stefan cel Mare University of Suceava, Str. Universitatii 13, Corp B, 720229 Suceava, jud. Suceava, Romania*
E-mail: stelian.alaci@usm.ro
[b]*SciBuCom 2 Ltd., P.O.Box 249, 1113 Sofia, Bulgaria*
[c]*Faculty of Industrial Engineering, Tribology Centre, Technical University – Sofia, 8 Kl. Ohridski Blvd., 1000 Sofia, Bulgaria*
[d]*South Ural State University, 76 Prospekt Lenina, Chelyabinsk, Russia*

Abstract. Polyurethane foams are broadly used in various applications, from domestic items to aero-spatial and medical devices. Knowledge of the damping characteristics of the materials is a necessity, both for the classic ones who due to ageing suffer changes of behaviour and for the newly developed, eco-friendly materials. In the present work, the polyurethane foam is modelled as an assembly between a nonlinear elastic element and a dashpot, in parallel. This material is subjected to impact by the metallic bob of a mathematical pendulum. For the completed dynamic system, the mathematical model is developed for finding the characteristic parameter of damping. There are also presented the experimental methods for achieving the constants from the dynamical equation of the model: the elastic parameters of static loading, the impact velocity and the coefficient of restitution. The theoretical model should be validated: the signal provided by an accelerometer sensor attached to the bob is interpolated by the signal given after the integration of the dynamical equation and a very good agreement is obtained. The expedite manner and the low cost are the main advantages of the method.

Keywords: polyurethane foams, dynamic model, experimental set-up, hysteresis.

AIMS AND BACKGROUND

Polyurethanes foams are a family of flexible synthetic polymers wished for varied applications from automotive, robotics, shoe industry, building construction, packaging, domestic application and medicine. There are well known the wear effects produced by vibrations[1] and so, anti vibration dampers are nowadays research domain. Reprocessing of these foams is difficult and costly and due to the recycling complications, they are cast-off after being used, generating contamination problems of environment[2]. Biological degradation of polyurethanes is an advanced research domain as it contributes to the design of eco-friendly materials sensitive to biodegradation phenomena and the progress of green recycling methods[3,4].

* For correspondence.

Therefore, new materials are required, with improved recycling capability, like new biodegradable polyurethane foams[5]. A type of new materials is the bio-based materials (lignin, starch) whose manufacturing requires awareness of the processing and material properties of the polymers. But the resulting properties of bio-based materials should be equal or be better than those of the conventional alternatives[6]. The chemical structure of polyurethane, either classical or biodegradable, modifies during ageing phenomenon. Laborious researches are made in dynamical, tensile, fatigue tests for controlling the effect of ageing: the Young modulus decrease, strength decrease, variation of stiffness[7]. An additional methodology, aiming to describe rapidly the damping characteristics of the polyurethane material is proposed in the present paper.

The main characteristic of two bodies which collide is the sudden variation of the kinematical parameters with the high forces development as the direct consequence. With the purpose of estimate these forces, the hypothesis of deformable bodies is essential. The relative deformation between the two nonconforming bodies is defined as the distance between the two points outlining the initial contact of the two bodies; this distance increases from zero up to a maximum value x_{max} and after that (when no plastic deformations occur), progressively decreases to zero and now the collision is finished[8]. The instant corresponding to the maximum value of normal approach separates the impact period into two phases, the compression and the restitution (Fig. 1). The maximum deformation is reached at the time t_c and therefore the relative velocity between the bodies is zero. A major parameter used in the study of impact is the coefficient of restitution c_r, defined as the negative ratio between the after and before relative velocities for the centric collision of two balls[9]:

$$c_r = -(v'_2 - v')/(v_2 - v). \tag{1}$$

When one of the bodies is immobile, for instance, the body 2 in Fig. 1, and takes the form:

$$c_r = -v'_1/v_1. \tag{2}$$

The study of impact requires applying the momentum theorem:

$$m_1 v_1 + m_2 v_2 = m_1 v'_1 + m_2 v'_2 \tag{3}$$

which, together with relation (1), allows for finding the post impact velocities of the bodies. A more difficult task is to obtain the relation of variation of the impact force during the period of collision. Supplementary hypothesis concerning energetic aspects must be considered.

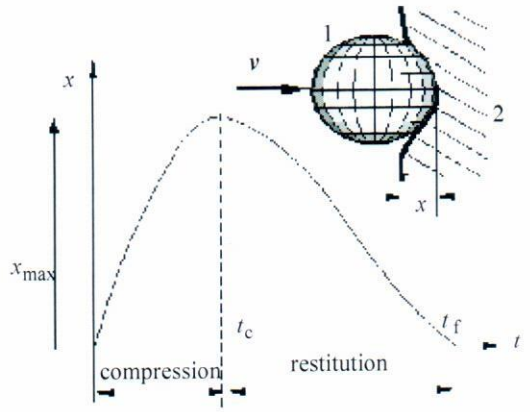

Fig. 1. Variation of normal approach of the bodies during the impact period

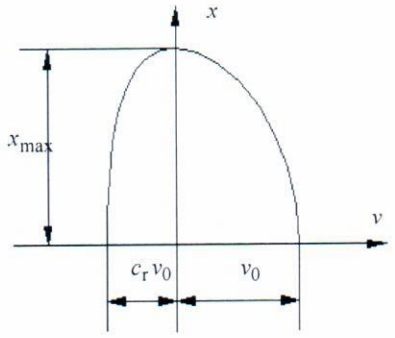

Fig. 2. Phase diagram

A first model was proposed by Hunt and Crossley[10] who regarded the impacting balls as viscoelastic bodies and proposed the impact force as the sum of an elastic term:

$$F_e = Kx^{3/2} \tag{4}$$

and a viscoelastic damping term:

$$F_d = c\dot{x}. \tag{5}$$

Hunt and Crossley show that the model depicted by a hysteresis curve closed in origin needs a coefficient c proportional to the elastic force, thus the damping force takes the form:

$$F_a = \chi x^{3/2}\dot{x}, \tag{6}$$

where the constant χ characterises the damping phenomenon. Another model is due to Lankarani[11] who considers a viscoelastic impact model and equals the lost

energies by damping during the two phases of the collision phenomenon. For the χ coefficient proposes the relation:

$$\chi = 3K(1 - c_r^2)/(4v_0). \tag{7}$$

The Lankarani model is appropriate only for collisions with $c_r > 0.9$, known also as quasielastic collisions. Following the Hunt and Crossley model, Flores[12] builds the viscoelastic model of impact accepting that, the path of the characteristic point in the phase plane is a quarter of ellipse both for compression and restitution periods, with the same major axis but different minor axes, as represented in Fig. 2. He finds for the damping coefficient the next expression:

$$\chi = 8K(1 - c_r)/(5c_r v_0). \tag{8}$$

The Flores model is suitable for the whole range of the coefficients of restitution, $0 < e < 1$.

The present paper proposes a model for the impact between a rigid punch and a foam type material, by broadening the Flores model. For the experimental researches, polyurethane foam was used. If for the Lankarani and Flores models, the impact of metallic materials led to negligible dimensions of the contact area, for the polyurethane the deformations are comparable to the dimensions of the body. Another significant difference between the two types of materials is the fact that, for the static contact, the loading and unloading characteristics are identical for metals but for the polyurethane foam[13], the two curves differ: the loading is performed via a power law curve described by:

$$F_c = Cx^{\alpha}. \tag{9}$$

With the α exponent:

$$1 \leq \alpha < 3/2 \tag{10}$$

while the unloading is accomplished in the elastic domain obeying the relation:

$$F_r = C'x^{3/2}. \tag{11}$$

The dynamic model for the impact is presented next. The impact force results from an elastic force, relation (9) to which a damping force, relation (6) is added. For the restitution phase, the exponent has the value[9] $\alpha_2 = 3/2$:

$$F = -\begin{cases} C_1 x^{\alpha_1} + \chi x^{\alpha_1}\dot{x}, & 0 \leq t \leq t_c \\ C_2 x^{\alpha_2} - \chi x^{\alpha_2}\dot{x}, & t_c \leq t \leq t_f \end{cases} \tag{12}$$

When the compression phase ends, the velocity is zero and the deformation reaches the maximum value x_{max}. The continuity condition imposed to the force at the instant t_c is expressed as:

$$C_1 x_{max}^{\alpha_1} = C_2 x_{max}^{\alpha_2}. \tag{13}$$

The Flores hypothesis is considered and the characteristic point moves in the phase plane on quarter ellipses. The velocity of the ball before impact is denoted by v_0 and the variation of the modulus of velocity for the two phases results under the form:

$$v(x)=\begin{cases} v_0\sqrt{1-(x/x_{\max})^2}, & 0\le t\le t_c \\ c_r\sqrt{1-(x/x_{\max})^2}, & t_c\le t\le t_f \end{cases} \tag{14}$$

The energy theorem is applied for the compression phase:

$$\int_0^{x_{\max}} C_1 x^{\alpha_1}\,dx+\int_0^{x_{\max}} \chi x^{\alpha_1} v_0\sqrt{1-(x/x_{\max})^2}\,dx=\frac{1}{2}mv_0^2, \tag{15}$$

and for the entire collision period:

$$\begin{aligned}&\int_0^{x_{\max}} C_1 x^{\alpha_1}\,dx+\int_0^{x_{\max}} \chi x^{\alpha_1} v_0\sqrt{1-(x/x_{\max})^2}\,dx+\int_{x_{\max}}^0 C_2 x^{\alpha_2}\,dx \\ &+\int_{x_{\max}}^0 -\chi x^{\alpha_1} c_r v_0\sqrt{1-(x/x_{\max})^2}=\frac{1}{2}(1-c_r^2)mv_0^2\end{aligned} \tag{16}$$

The next notation is introduced:

$$I(\alpha)=\int_0^1 \xi^{\alpha}(1-\xi^2)^{1/2}\,d\xi = 1/2\ B(\alpha/2,\ 1), \tag{17}$$

where $B(x, y)$ is the Euler integral of first kind. Taking into account relation (13), equations (15) and (16) provide the following equations:

$$\left[\frac{C_1}{\alpha_1+1}+\chi v_0 I(\alpha_1)\right]x_{\max}^{\alpha_1+1}=\frac{1}{2}mv_0^2, \tag{18}$$

$$\left[\frac{C_1}{\alpha_1+1}+\chi\, v_0 I(\alpha_1)\right]x_{\max}^{\alpha_1+1}-C_1\frac{x_{\max}^{\alpha_1+1}}{\alpha_2+1}+\chi\, x_{\max}^{\alpha_2+1}c_r v_0 I(\alpha_2)=\frac{1}{2}mv_0^2(1-c_r)^2 \tag{19}$$

The above equations form a system of equations with $x_{\max}$ and χ as unknowns. Solving the first equation with respect to χ and introducing it in the second equation, a transcendent equation as function of $x_{\max}$ is obtained:

$$\frac{1}{2}c_r mv_0^2\left[c_r+x_{\max}^{\alpha_2-\alpha_1}\frac{I(\alpha_2)}{I(\alpha_1)}\right]=\left[\frac{x_{\max}^{\alpha_1+1}}{\alpha_2+1}+\frac{x_{\max}^{\alpha_2+1}}{\alpha_1+1}\frac{I(\alpha_2)}{I(\alpha_1)}c_r\right]C_1 \tag{20}$$

The unknown $x_{\max}$ depends on C_1, α_1, v_0 and c_r. With these parameters stipulated, from equation (20) $x_{\max}$ is obtained by applying a numerical procedure. Next, via equation (18), the damping coefficient χ is found:

$$\chi = \left(\frac{1}{2} m v_0^2 - C_1 \frac{x_{\max}^{\alpha_1 + 1}}{\alpha_1 + 1} \right) \Big/ x_{\max}^{\alpha_1 + 1} v_0 I(\alpha_1) \tag{21}$$

EXPERIMENTAL

Equations (20) and (21) reveal that a complete characterisation of the impact phenomenon requires precising the values of the parameters C_1, α_1, v_0 and c_r. The values of these constants should be given as results from experimental work since other independent equations cannot be formulated. The experimental set-up designed for the study is presented in Fig. 3. The main part of device is a mathematical pendulum built from a prismatic body and two identical steel balls, attached symmetrically. A piezoelectric 3-axis accelerometer sensor[14] (range $3g$) is mounted on a face of the prism and the output signal is the input for a digital oscilloscope Tektronix TBS1000. The pendulum is at rest and the target, a prismatic polyurethane body is brought into contact to it (Fig. 3). The test consists in moving the pendulum in the vertical oscillation plane up to a mark from the working board, then letting it free to perform a succession of collisions with the target by one of the steel balls. In Fig. 4 is presented the schematics for the calculus of the initial impact velocity v_0 and the coefficient of restitution c_r. To this end, at initiation of the test, the bob of the pendulum (prism and balls) is moved with an angle θ with respect to the vertical and with a distance d on horizontal direction, respectively. The massless parallel wires materialise the rod of the pendulum.

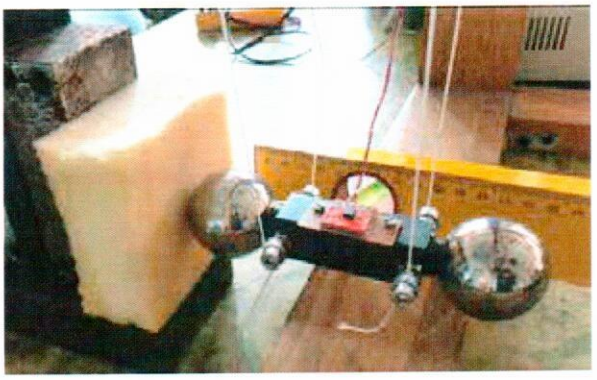

Fig. 3. Experimental pendulum

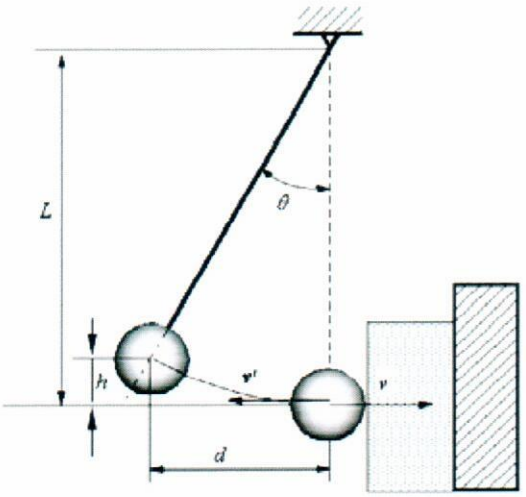

Fig. 4. Schematics for the calculus of the impact velocity and coefficient of restitution

Fig. 5. Needle attached to the prism indicates the position of the bob

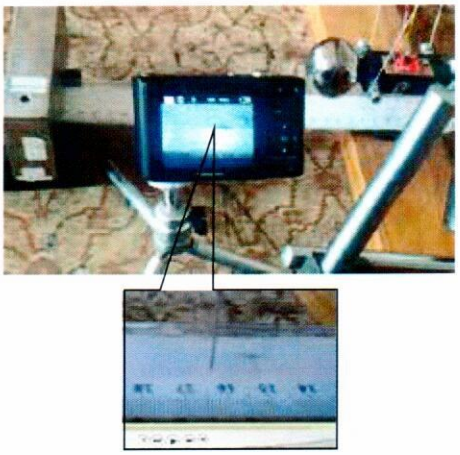

Fig. 6. Pendulum after rebound

Denoting by L the length of the rod, the angular elongation is given by:

$$\Theta = \text{asin}(d/L). \tag{22}$$

The position on vertical of the centre of the bob is denoted h and results as function of distance d:

$$h = L - L\cos\theta = L - L(1 - \sin^2\theta)^{1/2} = L - L(1 - (d/L)^2)^{1/2} = L - (L^2 - d^2)^{1/2}. \tag{23}$$

The energy theorem is applied for the moments of launching and impact initiation:

$$mgh = mv^2/2. \tag{24}$$

The initial impact velocity results from equations (23) and (24):

$$v_0 = v = (2gh)^{1/2} = (2g(L - (L^2 - d^2)^{1/2}))^{1/2}. \tag{25}$$

After impact, the centre of the bob performs the maximum rebound described by d' with respect to the initial un-deformed surface of the target, and the post-impact velocity can be calculated in a similar manner as:

$$v' = (2g(L^2 - d'^2)^{1/2}))^{1/2}. \tag{26}$$

Now, with known velocities v and v', the coefficient of restitution can be obtained:

$$c_r = \frac{(1 - (1 - (d'/L)^2)^{1/2})^{1/2}}{(1 - (1 - (d/L)^2)^{1/2})^{1/2}}. \tag{27}$$

A steel needle bonded to the prism moves along a ruler and permits the estimation of the distances d and d' (Fig. 5). The bob is brought into contact with a plane surface stopper (Fig. 6), for the launching position. The difference between the needle indications for start and rest positions (Fig. 5) gives the d parameter. A series of launchings are performed for a qualitative estimation of the rebound position. In the vicinity of this place, a video camera is set and the motion of the bob is recorded after launching it from a stipulated position d. The movie is split into frames and the instant when the sense of the motion changes is precisely identified and now the d' parameter is accurately estimated.

RESULTS AND DISCUSSION

The characteristic curve for quasi-static loading-unloading of a polyurethane foam can be obtained[13]; the test-rig and the methodology refer to two situations: flat and spherical punch. For the spherical punch, the steel balls $\Phi = 40$ mm are the same as the ones used in the bob of the pendulum. The experimental variation normal force-normal approach between spherical punch and parallelepiped foam is given in Fig. 7 in Cartesian coordinates and in Fig. 8 in logarithmic coordinates.

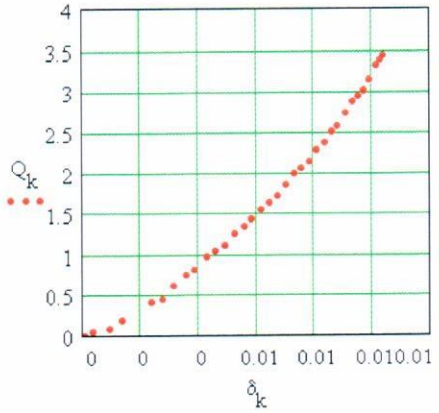

Fig. 7. Force-deformation curve for loading test (Cartesian coordinates)

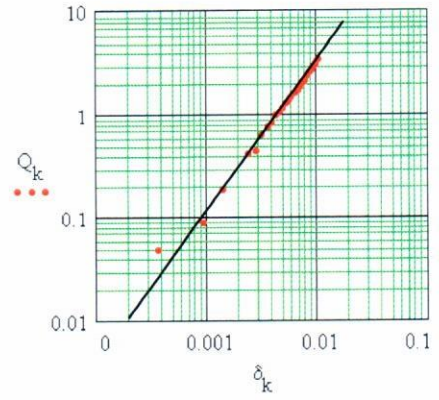

Fig. 8. Force-deformation curve for loading test (double logarithmic coordinates)

The experimental points from Fig. 8 lay on a straight line and confirm a dependency of the form:

$$\ln F = \ln C_1 + \alpha_1 \ln x. \tag{28}$$

Equation (28) expressed in Cartesian coordinates is:

$$F = C_1 x^{\alpha_1}. \tag{29}$$

The above expression was accepted as hypothesis in relation (9) and thus, the experimental work validates the hypothesis of the model. The parameters C_1 and α_1 are identified after applying the least squares method to the data in Cartesian coordinates. The objective function is:

$$f(C_1, \alpha_1) = \sum_k (Q_k - C_1 \delta_k^{\alpha_1})^2. \tag{30}$$

The condition of minimum is imposed to function (30), mathematically expressed as a system:

$$\begin{cases} \dfrac{\partial f(C_1, \alpha_1)}{\partial C_1} = 0 \\ \dfrac{\partial f(C_1, \alpha_1)}{\partial \alpha_1} = 0 \end{cases} \tag{31}$$

The explicit form of the system (31) is:

$$\begin{cases} -2\left[\sum_k Q_k \delta_k^{\alpha_1} - C_1 \sum_k \delta_k^{2\alpha_1}\right] = 0 \\ 2C_1\left[\sum_k C_1 \delta_k^{2\alpha_1} \ln \delta_k - \sum_k Q_k \delta_k^{\alpha_1} \ln \delta_k\right] = 0 \end{cases} \tag{32}$$

The numerical solving is the only possible method in solving the system (32) and a guess value is required. Since there is the possibility of multiple solutions, this requirement is a difficult task. Additionally, for the parameter C_1, the single information is $C_1 > 0$; for α_1 the range is known, according to equation (10). To surpass this difficulty, the notice that the first equation of the system (32) can be solved with respect to C_1 is applied. Replacing this solution into the second equation of the system, the next transcendental equation results:

$$f(\alpha_1) = \sum_k \frac{\sum_k Q_k \delta_k^{\alpha_1}}{\sum_k \delta_k^{2\alpha_1}} \delta_k^{2\alpha_1} \ln \delta_k - \sum_k Q_k \delta_k^{\alpha_1} \ln \delta_k \tag{33}$$

Function (33) plotted for the domain [1–2.5] is presented in Fig. 9 where a unique solution α_1 is obvious. This solution is used in finding the constant C_1 from the first equation (32) and then the interpolation curve of the experimental data is presented in Fig. 10.

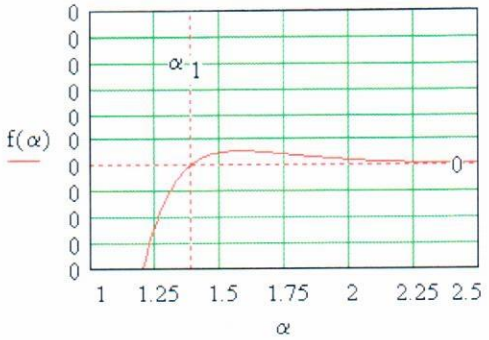

Fig. 9. Numerical solution for the exponent of the loading curve

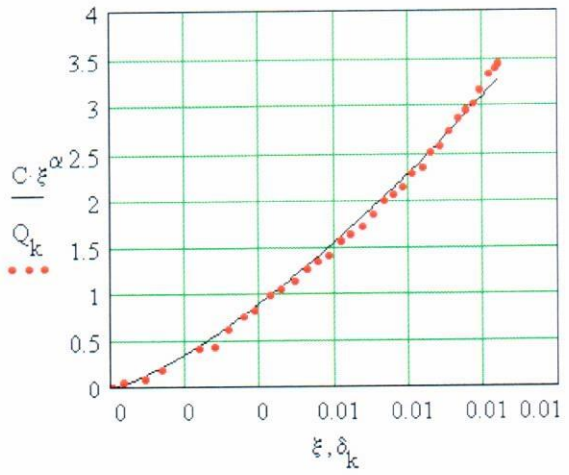

Fig. 10. Experimental data and the power interpolation curve

For the experimental data (Fig. 10), for loading characteristic, the values of the parameters are found $\alpha_1 = 1.32$, $C_1 = 2510$ N/m$^{\alpha 1}$. The impact initial velocity and the coefficient of restitution are calculated for the length of the rod of the pendulum $L = 1$ m and the displacements $d = 0.25$ m, $d' = 0.203$ m, resulting $v_0 = 0.8$ m/s and $c_r = 0.81$. From equation (20), the maximum approach is calculated $x_{max} = 0.024$ m and the coefficient of damping results applying equation (21) is $\chi = 1395$ (N/m$^{\alpha 1+1}$)/(m/s).

The definition of velocity:

$$v = \mathrm{d}x/\mathrm{d}t, \tag{34}$$

conducts to the differential equation:

$$\mathrm{d}t = \mathrm{d}x/v(x). \tag{35}$$

Using equation (14), relation (35) is integrated for the compression phase and the value of t_c is obtained:

$$t_c = \int_0^{x_{max}} \mathrm{d}x/v(x) = \int_0^{x_{max}} \mathrm{d}x/(v_0(1-(x/x_{max})^2)^{1/2}) = \pi x_{max}/(2v_0) = 0.047 \text{ s}. \tag{36}$$

In an analogous manner, for the restitution phase, the time of rebound is found as:

$$t_r = \int_{x_{max}}^{0} \mathrm{d}x/v(x) = -\int_{x_{max}}^{0} \mathrm{d}x/(c_r v_0(1-(x/x_{max})^2)^{1/2}) = \pi x_{max}/(2c_r v_0) = 0.059 \text{ s}. \tag{37}$$

Therefore, the total impact period is:

$$t_f = t_c + t_r = \pi x_{max}(c_r + 1)/(2c_r v_0) = 0.106 \text{ s}. \tag{38}$$

At this stage, the expression of the force acting in contact given by equation (12) is fully known. The equation of motion of the bob is a nonlinear differential equation of second order:

$$m\ddot{x} = -\begin{cases} C_1 x^{a1} + \chi x^{a_1}\dot{x}, & 0 \le t \le t_c \\ C_2 x^{a2} - \chi x^{a_2}\dot{x}, & t_c \le t \le t_f \end{cases} \tag{39}$$

Equation (39) is integrated using the Runge-Kutta IV method[15]. The time variations for approaching, velocity, acceleration (and force, implicit) are found (for the mass of the bob $m = 0.75$ kg) and shown in Figs 11–13. The phase plane is plotted in Fig. 14 and the hysteresis curve resulting from the force-deformation characteristic – in Fig. 15.

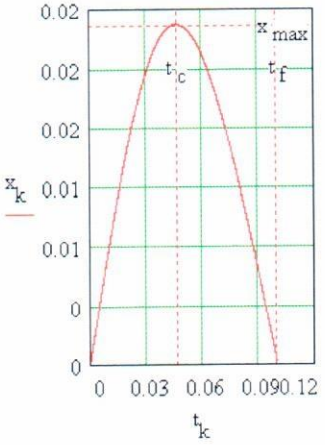

Fig. 11. Approach versus time during contact period

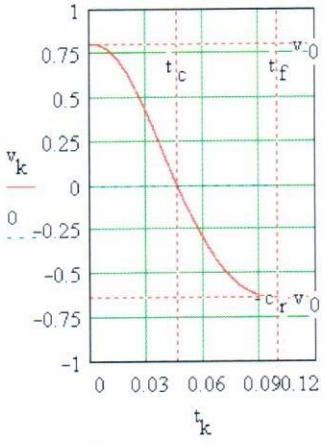

Fig. 12. Impact velocity during contact period

In Fig. 14, beside the characteristic curve from the phase plane obtained by the integration of the equation of motion, the velocity from the Flores model[12] was also plotted. It is noticed that for the compression phase ($v > 0$) there is excellent correlation but for the restitution phase ($v < 0$) there is an observable difference. The consequence of this difference can be also noticed in the graph of variation of acceleration (Fig. 13), where a slope discontinuity (marked by an arrow in the plot) is present.

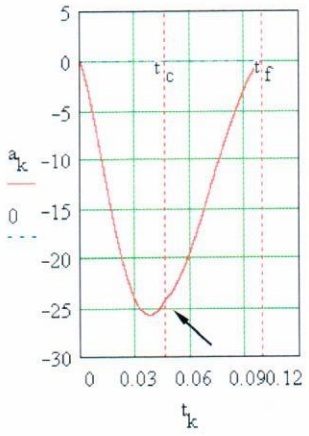

Fig. 13. Acceleration during contact period

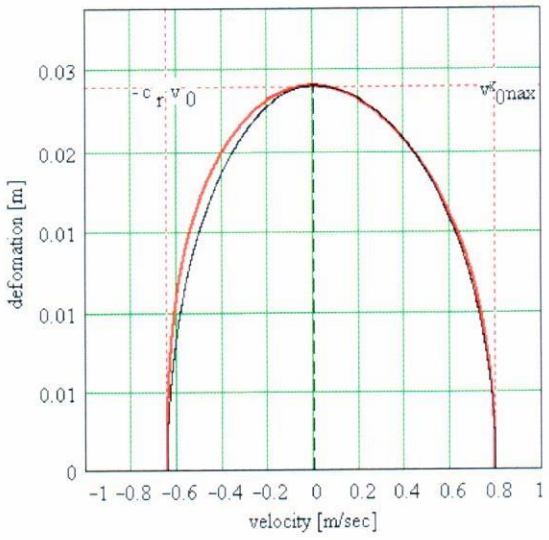

Fig. 14. Phase plane (black-solution of equation of motion; red-Flores model)

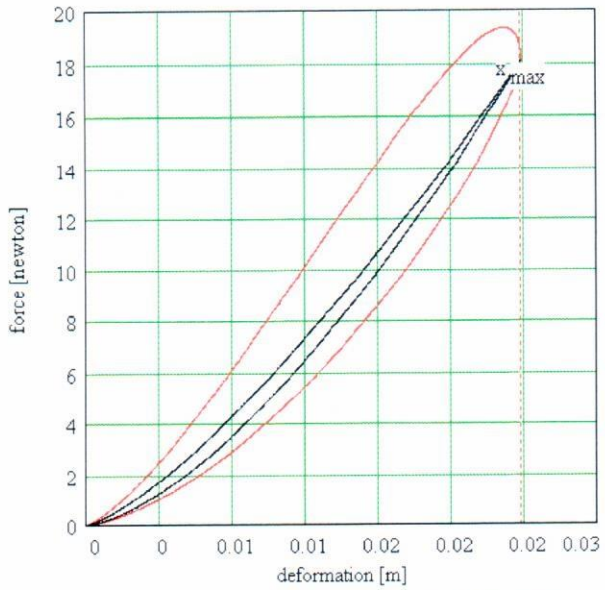

Fig. 15. Force-deformation plot, evidencing the hysteresis loop (black-static)

In order to validate the theoretical model, the experimental signal given by the accelerometer sensor was received by the digital oscilloscope (Figs 16 and 17), and saved as matrix. The experimental points for the first impact, the signal from Fig. 17, were interpolated using the theoretical signal given by the equation of motion. The two results are presented overlapped in Fig. 18 and an excellent approximation is obtained for the compression phase but also a good agreement for the restitution phase, which can be improved using a more sophisticated method for the characteristic curve.

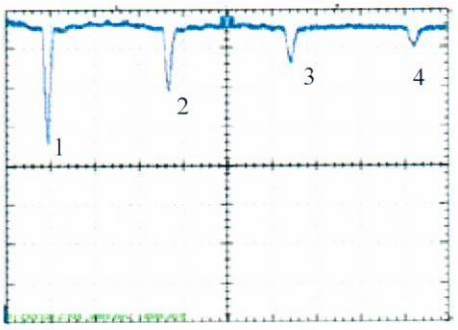

Fig. 16. Signal obtained at the oscilloscope for the first four collisions

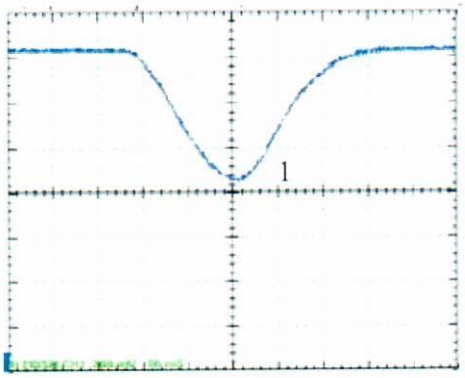

Fig. 17. Detail of signal for the first collision

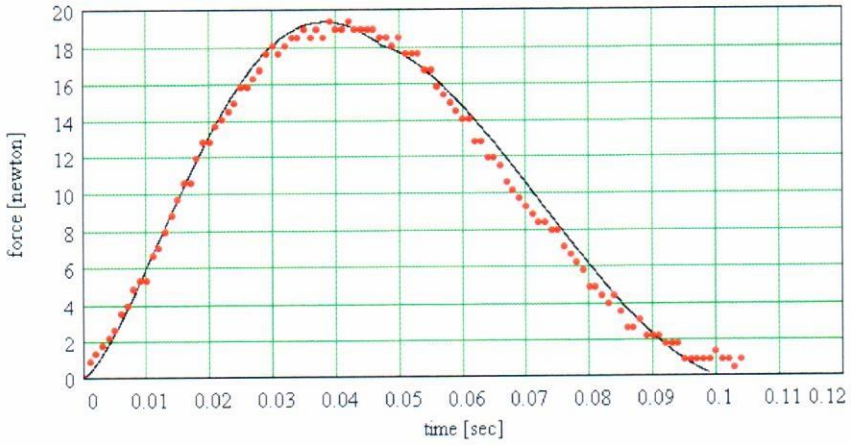

Fig. 18. Experimental data interpolated with the theoretical signal

CONCLUSIONS

The paper proposes a theoretical impact model for the foam type materials. The model considers the hypothesis that the impact force has two components: an elastic one and a viscous damping one. The Flores assumption is employed, the path of the characteristic point in the phase plane follows elliptic quarter for both impact phases. For the quasi-static loading the power-law dependency between force and deformation is accepted. Based on these hypotheses, a model is developed, allowing for finding the maximum approach, the coefficient of damping and the impact time and additionally, the hysteresis curve closes in origin. An experimental set-up was designed and employed, consisting principally in a mathematical pendulum with attached accelerometer. The device permits the estimation of the amplitudes during the impact used in calculating the initial and final impact velocities and implicitly of the coefficient of restitution which are required by the theoretical

model. From experiments and additional calculus, all the parameters involved in the nonlinear differential equation of the model describing are known. This equation is numerically integrated and permits representing the time dependencies for the approaching between bodies, contact velocity and acceleration. Next, these relations are used for plotting the characteristic curves from the phase plane and the force-deformation curve with hysteresis loop emphasised. The output signal from the accelerometer is collected by the memory oscilloscope and thus the impact force variation in time is experimentally obtained. It is observed that the curve generated with the theoretical model interpolates in a very good manner the experimental data.

REFERENCES

1. M. KANDEVA, T. GROZDANOVA, D. KARASTOYANOV, B. IVANOVA, K. JAKIMOVSKA, A. VENCL: Wear under Vibration Conditions of Spheroidal Graphite Cast Iron Microalloyed by Sn. J Balk Tribol Assoc, **22** (2A-1), 1310 (2016).
2. J. DAVID, L. VOJTOVA, K. BEDNARIK, J. KUCERIK, M. VAVROVA, J. JANCAR: Development of Novel Environmental Friendly Polyurethane Foams. Environ Chem Lett, **8**, 381 (2010).
3. M. E. POLLET, V. PHALIP, L. AVÉROUS: Evaluation of Biological Degradation of Polyurethanes. Biotechnol Adv, 107457 (2019).
4. P. ATANASOAE, R. D. PENTIUC: Considerations on the Green Certificate Support System for Electricity Production from Renewable Energy Sources. Procedia Engineering, **181**, 796 (2017).
5. R. V. GADHAVE, P. A. MAHANWAR, P. T. GADEKAR: Lignin-Polyurethane Based Biodegradable Foam. Open J Polym Chem, **8,** 1 (2018).
6. M. POPA, A. MITELUT, P. NICULITA, M. GEICU, M. GHIDURUS, M. TURTOI: Biodegradable Materials for Food Packaging Applications. J Environ Protect Ecol, **12** (4), 1825 (2011).
7. A. TCHARKHTCHI, S. FARZANEH, S. ABDALLAH-ELHIRTSI, B. ESMAEILLOU, F. NONY, A. BARON: Thermal Aging Effect on Mechanical Properties of Polyurethane. Int J Polym Anal Ch (Taylor & Francis), **19** (7), 571 (2014).
8. S. ALACI, F. C. CIORNEI, C. FILOTE: Some Remarks upon Collision Between a Dropping Ball and a Rotating Disk. J Balk Tribol Assoc, **22** (2), 1560 (2016).
9. W. GOLDSMITH: Impact, the Theory and Physical Behaviour of Colliding Solids. Edward Arnold, Sevenoaks, 1960.
10. M. C. CIORNEI, S. ALACI, F.-C. CIORNEI, I.-C. ROMANU: Use of Loading-unloading Compression Curves in Medical Device Design. IOP-MSE, **227**, (012026) (2017).
11. P. FLORES, M. MACHADO, M. T. SILVA, J. M. MARTINS: On the Continuous Contact Force Models for Soft Materials in Multibody Dynamics. Mult Syst Dyn, **25,** 357 (2011).
12. H. M. LANKARANI, P. E NIKRAVESH: A Contact Force Model with Hysteresis Damping for Impact Analysis of Multibody Systems. J Mech Des, **112,** 369 (1990).
13. K. H. HUNT, F. R E. CROSSLEY: Coefficient of Restitution Interpreted as Damping in Vibroimpact. J Appl Mech, **7,** 440 (1975).
14. ***https://www.analog.com/media/en/technical-documentation/data-sheets/ADXL335.pdf.
15. J. H. MATHEWS, K. D. FINK: Numerical Method Using MATLAB. Prentice Hall, 1999.

Received 7 June 2020
Revised 24 July 2020